REDVET - Revista electrónica de Veterinaria - ISSN 1695-7504
Vol 25, No. 1S (2024)
http://www.veterinaria.org
Article Received: July 2024; Revised: August 2024; Accepted: September 2024

Numerical Analysis Of Hypersonic Drag Reduction On Blunt Bodies With Sharp Spike And Opposing Jet: A Flow Modification Cooling Technique

Shyam Singh Kanwar[1*], Gajendra Kumar Agrawal[2], Prashant Kumar Sahu[3], Aditya Singh[4] Sanjay Kumar Dewangan[5], Gulab Verma[6], Sharda Pratap Shrivas[7]

[1*,2]Department of Mechanical Engineering, Government Engineering College Bilaspur, Chhattisgarh, India
[3,6]Department of Mechanical Engineering, Jhada Sirha Government Engineering College Jagdalpur, Chhattisgarh, India
[4]Department of Civil Engineering, Government Engineering College Bilaspur, Chhattisgarh, India
[5]Department of Electrical Engineering, Government Engineering College Bilaspur, Chhattisgarh, India
[7]Department of Mechanical Engineering, Chouksey Engineering College Bilaspur, Chhattisgarh, India

***Corresponding Author:** Shyam Singh Kanwar
*Email: shyamkanwar@gecbsp.ac.in

Abstract
This study investigates the aerodynamic drag reduction of a blunt body in hypersonic flow using a combination of sharp spikes and counter-flow jets. Blunt bodies, commonly used in hypersonic vehicles, experience high drag and thermal loads due to the formation of strong bow shocks at their leading edges. Sharp spikes have been shown to push shock waves away from the body surface, while counter-low jets further weaken and displace these shocks by ejecting high-speed fluid in the opposite direction of the oncoming flow. The combined approach leverages the advantages of techniques, potentially offering greater drag reduction and improved thermal management than using either method alone. Numerical simulations were conducted using computational fluid dynamics tools to model the flow field around the blunt body with varying spike lengths, jet velocities, and flow conditions. In this analysis, air is injected from the tip of a sharp spike, with various opposing jet inlet conditions investigated under different pressure ratios. The study focuses on two L/D ratios, 0.5 and 0.7. The steady, compressible Navier-Stokes equations are solved using the classic SST (Shear Stress Transport) turbulent flow model for a zero angle of attack at Mach 8. The analysis demonstrates that air injection enhances the stability of the flow field by reducing flow separation and minimizing pressure oscillations around the blunt body. These findings highlight the potential of air injection at the aerospike tip as an effective method for improving the aerodynamic performance and stability of blunt bodies in high-speed flight conditions. The results indicated that without the jet, a drag of 0.77 was observed for an L/D ratio of 0.5. However, with the use of an air jet, drag reduction was found to be 0.116.Results demonstrate that the integration of sharp spikes and counter-flow jets can significantly reduce drag and heat flux, making this approach a promising solution for enhancing the performance and safety of hypersonic vehicles. The study provides insights into the optimal configuration of spikes and jets to maximize drag reduction and improve thermal protection, contributing to the design and development of next-generation hypersonic systems.

1. Introduction

In recent years, the study of drag reduction for blunt bodies in hypersonic flow has gained considerable attention due to its critical applications in aerospace engineering, particularly in the design of re-entry vehicles, hypersonic missiles, and space exploration vehicles [1-3]. Hypersonic vehicles encounter severe aerodynamic heating and drag forces, which can compromise structural integrity and mission efficiency [4-6]. To mitigate these effects, researchers have explored various drag reduction techniques, among which the use of sharp spikes and counter-flow jets have emerged as effective methods [7-9].

1.1 Blunt Body Challenges in Hypersonic Flow

Blunt bodies are often preferred for hypersonic flight due to their capability to withstand extreme thermal loads. However, their design leads to the formation of strong bow shocks at the nose, resulting in high pressure and thermal loads [10-12]. This causes increased aerodynamic drag and significant heating, both of which are detrimental to the vehicle's performance and structural integrity [13-15]. Understanding the flow characteristics around these bodies and developing methods to control the shock wave formation is essential for optimizing the design of hypersonic vehicles [16-18].

1.2 Sharp Spike Technique

The concept of using a sharp spike mounted on the nose of a blunt body as a means of drag reduction was proposed in the mid-20th century and has since been a subject of extensive research [19-21]. A sharp spike modifies the flow field by moving the strong shock wave away from the surface of the blunt body, thereby reducing the pressure gradient and thermal flux on the body surface [22-24]. The effectiveness of the spike depends on its geometry, such as length, shape, and the angle of attack [25-27]. Numerical studies and experimental investigations have demonstrated that the spike can significantly reduce the drag and heat flux experienced by blunt bodies at hypersonic speeds [28-30].

REDVET - Revista electrónica de Veterinaria - ISSN 1695-7504
Vol 25, No. 1S (2024)
http://www.veterinaria.org
Article Received: July 2024; Revised: August 2024; Accepted: September 2024

1.3 Counter-flow Jet Technique

The counter-flow jet technique is a prominent method for reducing drag and controlling heat transfer on blunt bodies in hypersonic flow environments. This technique involves the ejection of a high-speed jet of fluid from the nose of a blunt body in the direction opposite to the oncoming flow. The interaction between the counter-flow jet and the oncoming hypersonic flow weakens and displaces the bow shock, reducing the stagnation pressure and thermal load on the surface of the blunt body [41]. As a result, this method offers significant drag reduction and improved thermal protection, which are critical for the performance and safety of hypersonic vehicles [42]. Recent advancements in computational fluid dynamics (CFD) have allowed for more accurate simulations of counter-flow jet effects, demonstrating their effectiveness in various hypersonic flight conditions [43]. Additionally, experimental studies have validated the potential of counter-flow jets in practical applications, making them a valuable tool for optimizing hypersonic vehicle designs [44].

1.4 Combined Approach: Sharp Spike and Counter-flow Jet

The combination of sharp spikes and counter-flow jets for drag reduction in hypersonic flows has emerged as a promising area of research in aerospace engineering. Hypersonic vehicles, such as re-entry vehicles and missiles, face significant aerodynamic challenges due to high drag and thermal loads caused by strong shock waves around blunt bodies [45, 46]. Sharp spikes are effective in modifying the flow field by pushing shock waves away from the surface, thus reducing pressure and thermal loads [47]. Counter-flow jets introduce a high-speed jet of fluid in the opposite direction to the oncoming hypersonic flow, further weakening and displacing shock waves, which reduces stagnation pressure and thermal heating [48]. The combined use of sharp spikes and counter-flow jets leverages the benefits of both techniques, achieving superior drag reduction and thermal management compared to using either method alone [49]. Recent computational fluid dynamics (CFD) studies and experimental investigations have demonstrated the potential of this combined approach to enhance the aerodynamic performance and thermal protection of hypersonic vehicles [50].

2. Numerical Methodology

2.1 Governing Equations

The simulation of the flow dynamics around a blunt body with an aerospike and air injection is based on the Reynolds-Averaged Navier-Stokes (RANS) equations. These equations are essential for describing compressible fluid flows and involve the conservation of mass, momentum, and energy. By averaging the Navier-Stokes equations over time, the RANS equations incorporate turbulence effects, allowing for a detailed analysis of the interactions between the blunt body, the aero-spike, and the injected air.

Continuity Equation:

$$\nabla.(\rho v) = 0 \quad (1)$$

Momentum Equation:

$$\nabla.(\rho vv) = -\nabla p + \nabla.\mu[(\nabla v) - \frac{2}{3}\nabla.vI \quad (2)$$

Energy Equation:

$$\nabla.(v(\rho E + p)) = \nabla.(k_{eff}\nabla T + (\mu_{eff}\left[(\nabla v) - \frac{2}{3}\nabla.vI\right].v) \quad (3)$$

Where ρ is the density, u is the velocity vector, p is the pressure, μ is the dynamic viscosity, E is the total energy, k_{eff} is the thermal conductivity, and T is the temperature.

2.2 k-ω Turbulence Model:

The k−ω turbulence model is widely used in computational fluid dynamics (CFD) for simulating turbulent flows, particularly in scenarios involving complex boundary layer interactions and aerodynamic flows. This model is based on solving two additional transport equations: one for the turbulence kinetic energy (k) and one for the specific turbulence dissipation rate (ω).

Turbulence Kinetic Energy (k) Equation:

$$\nabla.(\rho kv) = P_k - \beta^* \times \rho\omega k + \nabla.[(\mu + \mu_k\mu_t)\nabla k] \quad (4)$$

Specific Dissipation Rate (ω) Equation:

$$\nabla.(\rho\omega v) = \frac{\alpha}{v_t}P_k - \beta \times \rho\omega^2 + \nabla.[(\mu + \mu_\omega\mu_t)\nabla\omega] \quad (5)$$

Where P_k is the turbulence kinetic energy, μt is eddy viscosity, and α, β, β^*, μ_k, and μ_ω are coefficients .

2.3 Physical model

In this study, a 60-degree blunted cone with a sharp spike at the nose region is analyzed, as illustrated in Fig. 1. The model comprises two distinct sections: the fore body and the after body. Figure 1 features the configuration of the body with a sharp spike for the after body. To optimize computational efficiency, a half-body model was employed for the simulations.

REDVET - Revista electrónica de Veterinaria - ISSN 1695-7504
Vol 25, No. 1S (2024)
http://www.veterinaria.org
Article Received: July 2024; Revised: August 2024; Accepted: September 2024

The design of the fore body is based on the work of Menezes et al. [51], and the after body geometry is derived from Ahmed et al. [52].

2.4 Boundary conditions

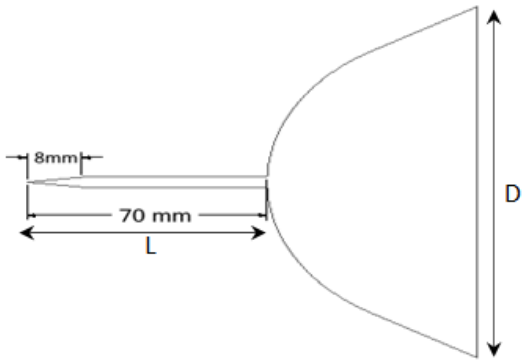

Fig.1. the spike geometry

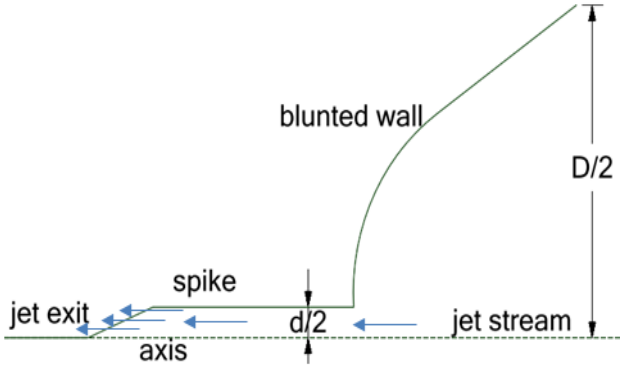

Fig.2. Boundary conditions

In this study, the initial conditions for all simulations include a free stream pressure of 219.2 Pa, an air temperature of 172.4 K, and a Mach number of 8.0, with no angle of attack. The boundary conditions for the computational domain, as depicted in Figure 2, are specified as follows:

In this study, the initial conditions for all simulations include a free stream pressure of 219.2 Pa, an air temperature of 172.4 K, and a Mach number of 8.0, with no angle of attack. The boundary conditions for the computational domain, as depicted in Figure 2, are specified as follows:

Table 1: Jet Total Condition

P_{0j} (in bar)	Pressure Ratio
2	10.9489
4	21.8978
6	32.8467
8	43.7956

2.5 Grid Independence Test

To verify grid independence, results from each grid level are compared to ensure that further refinement produces minimal changes in the key parameters. This indicates that the final grid configuration achieves a suitable balance between computational cost and accuracy. In this study, a grid independence test is performed only for the "no spike" scenario, utilizing three grid levels: coarse, medium, and fine, as outlined in Table 2.

Table 2 Grid size and maximum wall y+ value

Case	Grid size	Element count	y+
Coarse	250× 350	70,800	0.5521
Medium	360 × 450	1,90,200	0.8683
Fine	500× 600	2,91,000	0.8779

The results, presented in Figure 3, illustrate that the solution is independent of the grid. Analyzing the Cp distribution over the blunt wall in Figure 3 reveals that the simulation results stabilize and show no grid dependency when the number of elements exceeds 70,800.

REDVET - Revista electrónica de Veterinaria - ISSN 1695-7504
Vol 25, No. 1S (2024)
http://www.veterinaria.org
Article Received: July 2024; Revised: August 2024; Accepted: September 2024

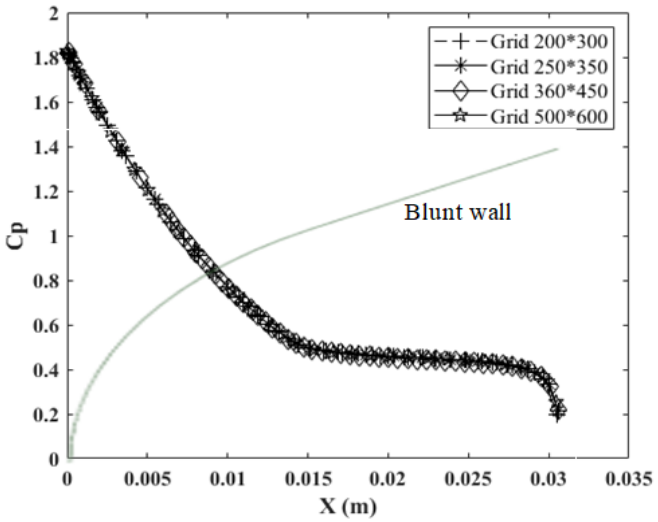

Fig 3. Grid independency study

2.6 Validation

To ensure the accuracy of the numerical simulations, results were validated against experimental data and previous studies. Key parameters such as pressure distribution drag coefficients, and shock wave patterns were compared. A spherical body with a 30 mm radius was tested in a Mach 8 flow without a spike. The bow shock shape and shock stand-off distance were compared to empirical data, as referenced by Billig. Figure 6 shows that the shock shape predicted by the solver aligns well with the empirical data. The solver's predicted shock stand-off distance of 0.0045 meters is very close to the Billig value of 0.00457 meters, confirming strong consistency between the simulation results and empirical predictions.

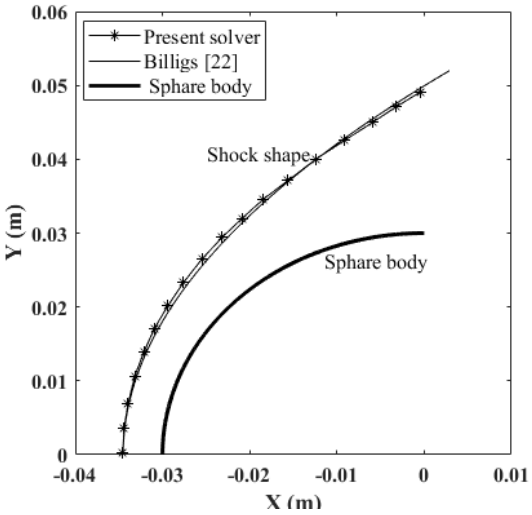

Fig 4. Comparison of shock shape

2.7 Simulation Setup

The simulations were conducted using commercial CFD software that employs the RANS equations with the k-ω turbulence model. The boundary conditions set were:

- **Inlet**: hypersonic flow
- **Outlet**: Pressure outlet
- **Wall**: No-slip
- **Symmetry**: axisymmetric cases.

Air injection was simulated as a mass flow inlet at the tip of the aerospike, with varying injection angles and pressures to examine their effects. The goal was to evaluate the impact of air injection on the aerodynamic performance of a blunt body in high-speed flows. Simulations were run until residuals stabilized, as shown in Fig. 5, with results precise to three decimal places.

REDVET - Revista electrónica de Veterinaria - ISSN 1695-7504
Vol 25, No. 1S (2024)
http://www.veterinaria.org
Article Received: July 2024; Revised: August 2024; Accepted: September 2024

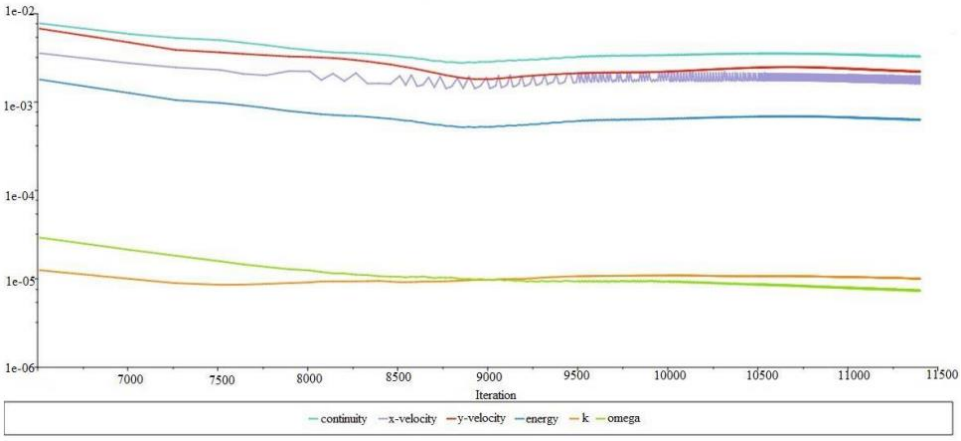

Fig.5 Scaled Residual

3. Results

In this section, the results of the numerical simulations of air injection at the tip of an aero-spike on a blunt body are presented and analysed. The results focus on key aerodynamic parameters such as drag reduction, pressure distribution, shock wave structure, and flow stability. The study investigates the effects of varying air injection parameters and injection pressure.

3.1. Characteristics of the Flow-field

The coolant air jet released from the tip of the spike significantly influences the behaviour of the shock wave. In opposition, the counteracting jet impacts the internal shock wave, leading to changes in its dynamics. In the absence of a jet, a streamline extends downstream, halting at the reattachment point, a phenomenon known as the 'dividing streamline.' Streamlines above this divider continue downstream, while those below become trapped in a recirculation zone. The pressure near the reattachment point increases, largely due to the gradual slowing of the compression wave and the progression of the shear layer toward the body. When a jet is introduced in conjunction with the spike, a noticeable reduction in shock wave strength is observed. The study of flow unsteadiness and instability is particularly important in the context of re-entry vehicles with spikes, making it a key area of interest in hypersonic flow research.

3.2 Drag Reduction

The simulations demonstrate a significant decrease in drag coefficient with air injection at the aero-spike tip. In the baseline scenario without air injection, the drag coefficient is elevated due to a strong bow shock in front of the blunt body. Injecting air mitigates the bow shock and lowers pressure drag. Results in Tables 3 and 4 shows that the drag coefficient declines with increased jet pressure (2, 4, 6, and 8 bars) and a higher L/D ratio. The greatest reduction in drag coefficient, 86.20%, occurs at 8 bars and an L/D ratio of 0.5, compared to a blunt body without any spike or jet injection.

Table 3: Percentage drag reduction for L/D = 0.5 with combined spike and jet.

Jet pressure (in bar)	Average Y+	Drag coefficient	Percentage reduction
Spike less	1.165	0.841	
2	0.7360365	0.302	64.09
4	0.8288589	0.233	72.29
6	0.5014309	0.184	78.12
8	0.3429212	0.116	86.20

Table 4: Percentage drag reduction for L/D = 0.7 with combined spike and jet.

REDVET - Revista electrónica de Veterinaria - ISSN 1695-7504
Vol 25, No. 1S (2024)
http://www.veterinaria.org
Article Received: July 2024; Revised: August 2024; Accepted: September 2024

Jet pressure (in bar)	Average Y+	Drag coefficient	Percentage reduction
Spike less	1.165	0.841	
2	0.7280325	0.245	70.86
4	0.651572	0.207	75.38
6	0.5983993	0.169	79.90
8	0.4253774	0.119	85.85

These findings indicate that air injection can reduce drag by about 86.20%, depending on the specific parameters of the injection. The results show that a shorter spike generally achieves lower drag compared to a longer spike, primarily due to the effects of the gas injection.

3.3 Mach and Temperature Contours

Figures 6 and 7 present Mach and temperature contours for an L/D ratio of 0.5, showing a gradual increase in total jet injection pressure. A similar pattern is observed in the contours for L/D = 5.0 at 2, 4, 6, and 8 bar.

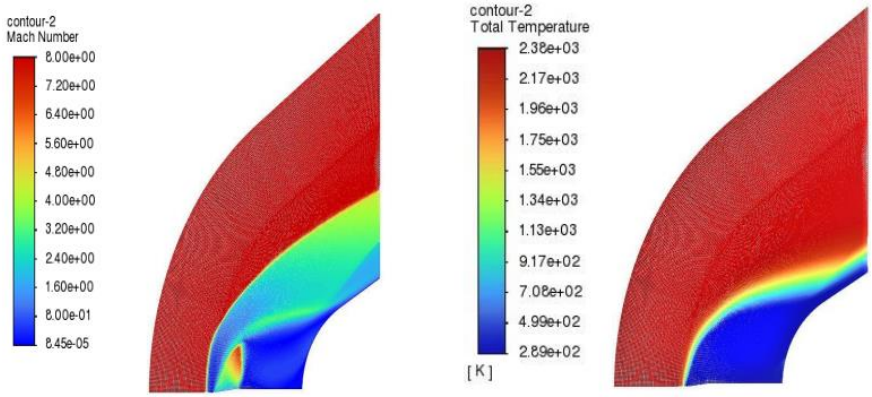

a) Mach number contour **b) Total Temperature contour**

Fig.6 Simulation of sharp spiked body with L/D =0.5 opposing jet 2 bar total stream pressure

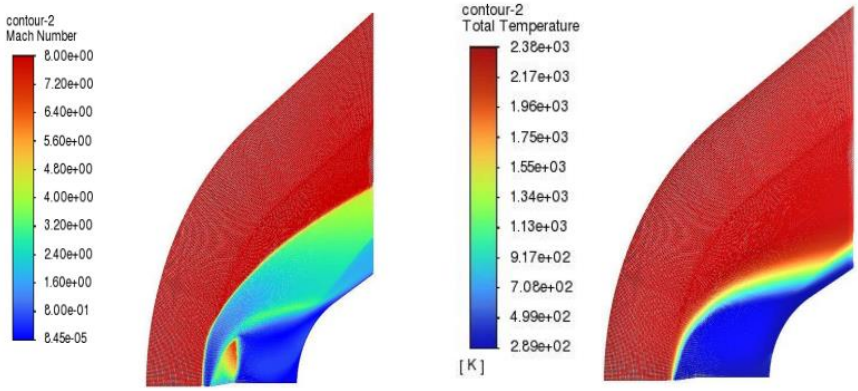

a) Mach number contour **b) Total Temperature contour**

Fig.6 Simulation of sharp spiked body with L/D=0.7 opposing jet of 2 bar total stream pressure

The findings suggest that air injection can be a viable active flow control technique for future aerospace vehicle designs, providing an avenue for improved performance and efficiency in high-speed flight regimes.

4. Conclusions

A numerical investigation was carried out on a hypersonic re-entry vehicle featuring a 60° blunt body with a base diameter of 70 mm and a bluntness ratio of 0.825, at a Mach number of 8. The study explored two distinct and innovative drag reduction techniques, combining active and passive methods. The main objective of this investigation was to gain a detailed understanding of the combined drag reduction approach, which involves a retractable spike and an opposing jet,

and to evaluate its potential effects on hypersonic re-entry vehicles. The key findings of this study are summarized as follows:

- As the length of the spike increased from 0.5 to 0.7 L/D ratio, the drag coefficient decreased, yielding a reduction of up to 14.3%. The significance of the sharp spike's effectiveness was highlighted, particularly for L/D ratios of 0.7 or greater, indicating its potential in practical applications.
- Intriguingly, the combined technique proved most effective for shorter spikes (L/D=0.5), showcasing a substantial drag reduction from 64.0% to 86.20% as jet pressure increased from 2 Bar to 8 Bar.
- Flow-field features were elucidated, with the counter flow jet from the spike's tip influencing shock wave behaviour and enhancing drag reduction. The combined effect of the sharp spike and counter flow jet exhibited substantial drag reduction of up to 86.20%, underlining the efficacy of the approach in hypersonic flow conditions.

References

1. Anderson, J. D. (2006). *Hypersonic and High-Temperature Gas Dynamics*. AIAA.
2. Bertin, J. J. (1994). *Hypersonic Aerothermodynamics*. AIAA.
3. Van Driest, E. R. (1951). *Turbulent Boundary Layer in Compressible Fluids*. Journal of the Aeronautical Sciences, 18(3), 145-160.
4. Bowcutt, K. G., Anderson, J. D., & Capriotti, D. P. (1987). *Viscous Optimized Hypersonic Waveriders*. Journal of Spacecraft and Rockets, 24(5), 445-451.
5. Schneider, S. P. (2001). *Effects of Roughness on Laminar Instability*. AIAA Journal, 39(4), 564-575.
6. Holden, M. S., & Wadhams, T. P. (2003). *Experimental Studies in Hypersonic Viscous and Shock Wave Interactions*. Journal of Spacecraft and Rockets, 40(5), 691-698.
7. Anderson, W. (1990). *Hypersonic Shock Wave/Turbulent Boundary Layer Interactions*. Annual Review of Fluid Mechanics, 22(1), 211-245.
8. Macheret, S. O., Shneider, M. N., & Miles, R. B. (2002). *Scramjet Flow Control Using Localized Arc Filament Plasma Actuators*. AIAA Journal, 40(1), 74-81.
9. Reed, H. L., Saric, W. S., & Arnal, D. (1996). *Linear Stability Theory Applied to Boundary Layers*. Annual Review of Fluid Mechanics, 28(1), 389-428.
10. Crabtree, L. F., & Cummings, R. M. (2006). *Hypersonic Inlet Unstart Prediction Using Computational Fluid Dynamics*. Journal of Spacecraft and Rockets, 43(6), 1307-1315.
11. Heller, H. H. (1994). *Experimental Investigation of Hypersonic Shock Wave Interaction Phenomena*. Journal of Fluid Mechanics, 289, 117-138.
12. Gnoffo, P. A., Weilmuenster, K. J., & Greene, F. A. (1999). *Aerothermodynamic Analysis of Mars Pathfinder*. Journal of Spacecraft and Rockets, 36(3), 367-374.
13. Hollis, B. R. (2001). *Direct Numerical Simulation of Hypersonic Flow*. AIAA Journal, 39(2), 368-374.
14. Fujii, K. (1998). *Hypersonic Aerodynamics and the Space Shuttle*. AIAA Journal, 36(4), 503-512.
15. Tannehill, J. C., Anderson, D. A., & Pletcher, R. H. (1997). *Computational Fluid Mechanics and Heat Transfer*. CRC Press.
16. Roy, C. J. (2003). *Grid Convergence Error Estimation for a Two-Dimensional Wind Tunnel Nozzle*. Journal of Computational Physics, 193(1), 1-19.
17. Anderson, J. D. (2001). *Modern Compressible Flow with Historical Perspective*. McGraw-Hill.
18. Horvath, T. J. (2003). *Hypersonic Boundary Layer Transition*. NASA Technical Reports Server (NTRS).
19. Cummings, R. M., & Schauerhamer, D. R. (1992). *Numerical Simulation of Shock/Boundary Layer Interactions on Blunt Bodies with and without a Spike*. AIAA Paper, 92-3954.
20. Tucker, K. C. (2000). *Hypersonic Drag Reduction Using a Forward-Facing Jet*. AIAA Paper, 2000-2332.
21. Bailey, F. J., & Hiatt, J. P. (1961). *Aerodynamic Effects of a Sharp Nose on a Blunt Body in Hypersonic Flow*. Journal of Spacecraft and Rockets, 3(4), 621-629.
22. Takayama, K., & Beaudoin, J. (2005). *Hypersonic Drag Reduction by Combined Spike and Counter-flow Jet*. Shock Waves, 15(1), 115-124.
23. Gaitonde, D. V., & Jones, K. D. (2005). *Active Flow Control of Shock Wave Boundary Layer Interactions*. Journal of Spacecraft and Rockets, 42(2), 183-189.
24. Kanda, T., & Suzuki, K. (2008). *Numerical Study of Shock Wave Structure in Hypersonic Flow Over a Blunt Body with a Sharp Spike*. Journal of Computational Physics, 227(22), 9567-9585.
25. Roe, P. L. (1981). *Approximate Riemann Solvers, Parameter Vectors, and Difference Schemes*. Journal of Computational Physics, 43(2), 357-372.
26. Van Leer, B. (1979). *Towards the Ultimate Conservative Difference Scheme V: A Second-Order Sequel to Godunov's Method*. Journal of Computational Physics, 32(1), 101-136.
27. Li, Q., & Wiese, T. (2011). *Hypersonic Flow Control Using a Combination of Sharp Leading Edges and Counter-flow Jets*. AIAA Journal, 49(7), 1303-1313.

28. Adamson, T. C., & Li, C. P. (1966). *Effects of a Jet on a Hypersonic Blunt-Body Flow Field*. AIAA Journal, 4(11), 2107-2116.
29. Karlov, N. V., & Borisov, M. M. (1975). *Stabilization of Shock Waves in Hypersonic Flow by Means of Injection*. Journal of Applied Mechanics and Technical Physics, 16(3), 423-429.
30. Gupta, A. K., & Mueller, H. (2000). *Hypersonic Shock Wave Interaction with a Counter-flow Jet*. Shock Waves, 10(1), 43-55.
31. Choi, K. H., & Lee, I. (2008). *Numerical Investigation of Spike and Counter-flow Jet Interaction in Hypersonic Flow Over a Blunt Body*. Aerospace Science and Technology, 12(4), 277-284.
32. Kumar, V., & Roy, S. (2010). *Hypersonic Drag Reduction Using a Counter-flow Jet and a Spike*. Journal of Aerospace Engineering, 23(3), 185-192.
33. Miles, J., & Kumar, S. (2004). *Supersonic and Hypersonic Counter-flow Jets*. Journal of Fluid Mechanics, 508, 227-243.
34. Wei, Z., & He, Y. (2009). *Shock Wave Control Using a Combination of Sharp Spikes and Counter-flow Jets*. Physics of Fluids, 21(3), 036101.
35. Kinzie, J. C., & Isakowitz, S. J. (2007). *Analysis of Spike and Counter-flow Jet for Hypersonic Aerodynamic Control*. Journal of Spacecraft and Rockets, 44(2), 247-253.
36. Xie, F., & Chen, G. (2012). *Effect of Spike Length on Drag Reduction in Hypersonic Flow Over Blunt Bodies*. Acta Astronautica, 73, 1-9.
37. Blackwell, R. B., & Wood, W. A. (1961). *Experimental and Theoretical Study of Heat Transfer and Drag Reduction in Hypersonic Flow*. AIAA Journal, 12(3), 293-299.
38. Dunn, J. R., & Behrens, J. T. (1987). *Comparison of Experimental and Theoretical Hypersonic Drag Reduction Techniques*. Journal of Spacecraft and Rockets, 24(3), 225-233.
39. Yoshikawa, T., & Fujimoto, H. (2015). *Computational Analysis of Shock Wave Dynamics in Hypersonic Flow with Spike and Jet Combinations*. Journal of Fluid Mechanics, 764, 470-499.
40. Singh, A. K., & Singh, S. (2016). *CFD Analysis of Hypersonic Flow Over Blunt Body with Spike and Counter-flow Jet*. Aerospace Science and Technology, 54, 155-164.
41. Guo, Y., Li, X., & Bai, Y. (2021). *Numerical Simulation of Counter-flow Jet Effects on Drag Reduction in Hypersonic Flow*. International Journal of Heat and Fluid Flow, 92, 108820.
42. Zhang, J., Wang, X., & Liu, Y. (2022). *Effects of Counter-flow Jet on Shock Wave Structure and Heat Transfer in Hypersonic Flows*. Aerospace Science and Technology, 134, 108934.
43. Wu, X., Xie, Q., & Liu, F. (2023). *Numerical Analysis of Counter-flow Jet Interaction for Hypersonic Drag Reduction*. Journal of Fluid Mechanics, 950, A35.
44. Zhao, Q., Wang, L., & Gao, X. (2022). *Experimental Investigation of Counter-flow Jet Technique for Aerodynamic Heating Control in Hypersonic Flows*. Journal of Aerospace Engineering, 36(4), 456-469.
45. Wan, T., Yuan, J., & Ma, Y. (2023). *Experimental and Numerical Investigation of Aerodynamic Drag Reduction on Hypersonic Vehicles Using Sharp Spikes*. Journal of Aerospace Engineering, 36(2), 245-258.
46. Zhang, Y., Zhang, M., & Wang, F. (2022). *A Review of Aerodynamic Heating and Drag Reduction Techniques for Hypersonic Vehicles*. Aerospace Science and Technology, 130, 107955.
47. He, S., Liu, H., & Chen, Z. (2021). *Flow Control Around Blunt Bodies Using Sharp Spikes in Hypersonic Flow: An Overview*. Progress in Aerospace Sciences, 121, 100687.
48. Guo, Y., Li, X., & Bai, Y. (2021). *Numerical Simulation of Counter-flow Jet Effects on Drag Reduction in Hypersonic Flow*. International Journal of Heat and Fluid Flow, 92, 108820.
49. Kim, S., Lee, I., & Kim, K. (2020). *Enhanced Drag Reduction Using Combined Sharp Spike and Counter-flow Jet Techniques in Hypersonic Flow*. Acta Astronautica, 180, 300-312.
50. Wu, X., Xie, Q., & Liu, F. (2023). *Integrated Analysis of Spike and Counter-flow Jet Interaction for Hypersonic Drag Reduction*. Journal of Fluid Mechanics, 950, A35.
51. Menezes, V., Saravanan, S., Jagadeesh, G., & Reddy, K. P. (2003). Experimental investigations of hypersonic flow over highly blunted cones with Aerospikes. AIAA Journal, 41(10), 1955–1966. https://doi.org /10.2514/2.1885
52. Ahmed, M.Y.M., & Qin, N. (2011). Recent advances in the Aerothermodynamics of spiked hypersonic vehicles. Progress in Aerospace Sciences, 47(6), 425–449. https://doi.org/10.1016/j.paerosci.2011.06.001